Journal of Dental Sciences 20 (2025) 292–301

Available online at www.sciencedirect.com

ScienceDirect

journal homepage: www.e-jds.com

Original Article

From gingiva to multiple organs in mice: The trace of *Porphyromonas gingivalis* via *in vivo* imaging

Xin-Yi Cheng, Pei-Hui Zou, Yi-Ming Ma, Yu Cai, Qiao Shi, Jia Liu*, Qing-Xian Luan**

Department of Periodontology, Peking University School and Hospital of Stomatology & National Center for Stomatology & National Clinical Research Center for Oral Diseases & National Engineering Research Center of Oral Biomaterials and Digital Medical Devices& Beijing Key Laboratory of Digital Stomatology & NHC Key Laboratory of Digital Stomatology & NMPA Key Laboratory for Dental Materials, Beijing, China

Received 28 June 2024; Final revision received 11 July 2024
Available online 20 July 2024

KEYWORDS
Bacteremia;
In vivo imaging;
Metabolic labeling;
Mice;
Periodontitis;
Porphyromons gingivalis

Abstract *Background/purpose:* Periodontitis is associated with systemic health. One of the underlying mechanisms is the translocation of periodontal pathogens, among which *Porphyromonas gingivalis* (*Pg*) is the most common. Here, we aimed to illustrate the biodistribution and dynamics of *Pg* from gingiva to multiple organs through blood circulation.
Materials and methods: Pg tagged by Cyanine 7 (Cy7-*Pg*) was injected into the gingiva of healthy and periodontitis mice. *In vivo* imaging system (IVIS) was applied to monitor the distribution of Cy7-*Pg* in multiple organs which were isolated at serial timepoints. Polymerase chain reaction (PCR) was conducted to determine the *Pg* DNA copies in the gingiva, blood and organs. Cy7-*Pg* in the gingiva and organs was also confirmed by frozen section staining. Furthermore, to figure out whether the bacteremia derived from oral-gut axis, mice received gavage of Cy7-*Pg*. Then the blood and organ samples were detected in the similar way as above.
Results: Intra-gingival injection induced larger amounts of Cy7-*Pg* accumulating in the gingiva of periodontitis mice ($P < 0.05$) as confirmed by above three methods. Twenty minutes after injection, *Pg* DNA copies in the blood of periodontitis group were 36.3-fold higher than healthy group ($P < 0.05$). IVIS results, combined with PCR and frozen sections, demonstrated periodontitis induced longer retention with higher amounts of Cy7-*Pg* in the periodontitis group. *Pg* was enriched more significantly in the liver for the longer duration than the kidney and pancreas.

* Corresponding author. Department of Periodontology, School and Hospital of Stomatology, Peking University, No. 22, Zhongguancun South Avenue, Haidian District, Beijing, 100081. China.
** Corresponding author. Department of Periodontology, School and Hospital of Stomatology, Peking University, No. 22, Zhongguancun South Avenue, Haidian District, Beijing, 100081. China.
E-mail addresses: dentistliujia@126.com (J. Liu), kqluanqx@126.com (Q.-X. Luan).

https://doi.org/10.1016/j.jds.2024.07.009

Conclusion: Our study showed *Pg*, which accumulated in the gingiva, could translocate through blood circulation to multiple organs with varied duration and amounts.

Introduction

Periodontitis is one of the leading causes of tooth loss in the world,[1] which is initiated by the dental microorganisms.[2] *Porphyromonas gingivalis* (*Pg*), the keystone pathogen, plays an important role in orchestrating the biofilm from homeostasis to dysbiosis thus exacerbating inflammation.[3] Besides destruction of the periodontium, periodontitis also correlates with systemic comorbidities,[4] for which the underlying mechanisms have not been clearly defined.

Translocation of periodontal pathogens is one of the pathogeneses linking periodontitis and the overall health. *Fusobacterium nucleatum* (*Fn*) and *Pg*, for the most common, have been identified in human[5,6] and animal organs[7,8] using polymerase chain reaction (PCR), DNA hybridization, and immunological methods. The translocation through blood circulation has been described by the clinical studies from 1960s to 2000s. Transient bacteremia possibly occurred following invasive dental procedures[9,10] such as scaling and tooth extraction, as well as daily oral activities[11,12] like tooth brushing and chewing. The duration of the bacteremia was generally within 15 min and the magnitude was likely associated with the amounts of plaque and the degree of gingival inflammation. However, neither the fate nor the destination of the bacteria has been mentioned, with lack of multi-organ studies. To address these issues, we intended to label *Pg* and track it *in vivo*.

Metabolic labeling and *in vivo* imaging pave the way to trace live bacteria in live creatures. The former is one of the fluorescent labeling methods, which has no impact on the bacteria viability and doesn't compromise in anaerobic environment.[13] Bacteria integrate chemically modified unnatural precursors or substrate analogues into their own cell structures via an endogenous biosynthetic machinery, where subsequently a fluorophore combines usually through click chemistry reaction. Metabolic labeling has been primarily applied to visualize gut microbiota,[14,15] yet not launched for oral bacteria. Therefore, in this study, we applied the methods to trace the spatio-temporal distribution following *Pg* injection *in vivo*.

Materials and methods

Metabolic labeling of *Pg*

Pg (ATCC 33277) was picked into 1 mL fluid brain-heart infusion (OXIFID, Basingstoke, UK) medium, comprising hemin, vitamin K_1 and N-azidoacetylgalactosamine-tetraacylated ($Ac_4GalNAz$, Aladdin, Shanghai, China) at the final concentration of 100 μM. At an OD_{600nm} = 1.0 (~7×10^9 CFU/mL), the cultures were centrifuged (8000 g, 5 min) and washed 3 times with phosphate buffered saline. The pellet was resuspended in 100 μL of a reaction mixture containing different concentrations of Cyanine 7-Dibenzocyclooctyne (Cy7-DBCO, Zancheng, Tianjing, China), and incubated for 2 h. Then the labeled bacteria were washed 3 times, and put on ice immediately for animal experiments. The methods about *in vitro* experiments of Cy7-*Pg* were described in Supplementary Information, which illustrated metabolic labeling didn't impact viability, immunomodulatory ability or toxicity.

Animals

A total of sixty 6-week-old male C57BL/6J wild-type mice were acquired from Experimental Animal Laboratory, Peking University Health Science Center. The experimental protocol was approved by Review Board and Ethics Committee of Peking University Health Science Center (PUIRB-LA 2023007).

The periodontitis mice (Cp) were ligated with 5–0 silk sutures at bilateral maxillary second molars for three weeks. The ligatures were checked every three days and retied if not in place. The control mice were only anaesthetized (Fig. 1A). Microcomputed tomography was applied to evaluate the effect of periodontitis model as described in the Supplementary Information.

Intra-gingival injection of Cy7-*Pg*

Mice were anaesthetized with intraperitoneal injection of sodium pentobarbital. The ligatures were removed before injection. The Cy7-*Pg* pellet was resuspended with 2% carboxymethylcellulose sodium (CMC). Ten microliters of Cy7-*Pg* (~1×10^9 CFU) were injected by the microsyringe (Feige, Shanghai, China) with the similar force through the sulcular/pocket epitheliums into the gingiva. Five sites at each side of maxillary palatal gingiva were injected with 1 μL per site: the center of the first, second and third molar and the two papillae. Cotton balls were placed around the teeth to absorb the spilled Cy7-*Pg* liquid and changed for clean ones once wetted through with blood or Cy7-*Pg* liquid. After the injection, the cotton balls were taken out and the oral cavity was cleaned up and dried (Fig. 1B).

In vivo tracking of Cy7-*Pg*

Nine mice were divided into three groups (Fig. 1C): the healthy control (the control group, n = 3), the healthy mice with Cy7-*Pg* injection (the control-*Pg* group, n = 3),

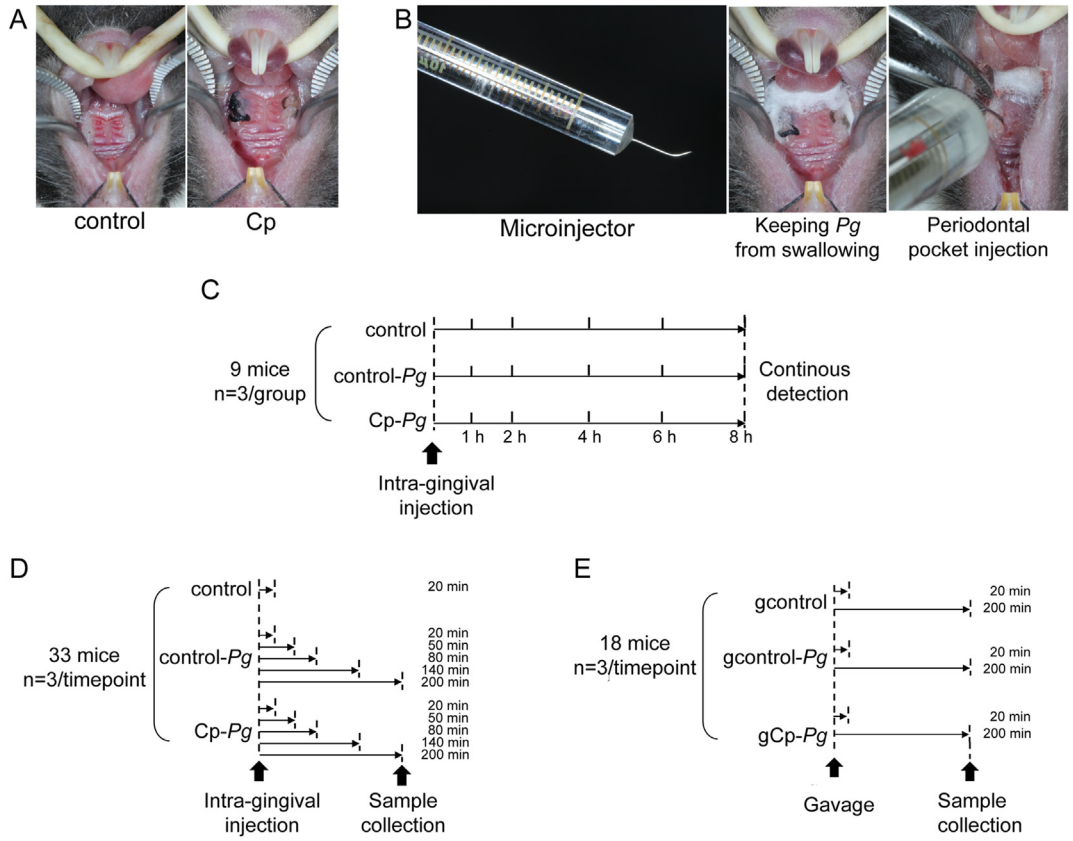

Figure 1 Study design

A: Intraoral photographs of healthy (the control group) and periodontitis mice (the Cp group). B: Intra-gingival injection of Cy7-*Pg* using a microinjector, with cotton balls around to absorb the spilled bacteria liquid. C: Detection of Cy7-*Pg* continuously for 8 h after intra-gingival injection. D: Distribution of Cy7-*Pg* in organs after intra-gingival injection. E: Distribution of Cy7-*Pg* in organs after oral gavage. control-*Pg*: the healthy mice with Cy7-*Pg* injection. Cp: periodontitis mice by ligature. Cp-*Pg*: the periodontitis mice with Cy7-*Pg* injection. Cy7-*Pg*: *Porphyromonas gingivalis* labeled by cyanine 7. gcontrol: the healthy mice with carboxymethyl cellulose gavage. gcontrol-*Pg*: the healthy mice with Cy7-*Pg* gavage. gCp-*Pg*: the periodontitis mice with Cy7-*Pg* gavage.

and the periodontitis mice with Cy7-*Pg* injection (the Cp-*Pg* group, n = 3). The control mice were only anaesthetized. All mice were dehaired and fasted overnight. After intra-gingival injection, mice were imaged for Cy7 detection using an *in vivo* imaging system (IVIS Spectrum, PerkinElmer, Waltham, MA, USA) at 1 h, 2 h, 4 h, 6 h and 8 h. Between the time points, the mice were returned to cages. The parameters were as below: fluorescent imaging; exposure time, 4 s; binning factor, 8; f-stop, 2; the field of view of C (13.4 cm). Excitation wavelength = 745 nm and emission wavelength = 800 nm. Photography parameters were as below: binning factor, 2; f-stop, 8. Data were analyzed with Living Image version 4.4 (Caliper Life Sciences, Hopkinton, MA, USA).

Another thirty-three mice were separated into the control group (n = 3), the control-*Pg* group (n = 15) and the Cp-*Pg* group (n = 15) (Fig. 1D). Following the Cy7-*Pg* injection, at 20 min, 50 min, 80 min, 140 min and 200 min (each group contained 3 mice at each time point), blood samples were collected by plucking eyeballs and mice were then euthanized. Multiple organs (the liver, kidney, pancreas and gastrointestinal tract) were isolated, and placed in the same order and position on the culture plate lids for IVIS (PerkinElmer) detection. The IVIS settings were the same as mentioned above. It cost 20 min to inject bacteria, collect blood samples and separate organs, therefore 20 min was set as the first timepoint. During the analysis, regions of interest (ROIs) were put on each organ of the fluorescent images, and average signal intensities were calculated within ROIs, which were in the same and suitable size and shape for each organ. The blood samples were kept at −80 °C for DNA extraction. The liver (20 min, 50 min, 80 min and 200 min), kidneys (50 min), pancreas (50 min) and gingiva (50 min) were harvested for DNA extraction and frozen sections. The methods for DNA extraction and frozen sections were described in Supplementary Information.

Oral gavage of Cy7-*Pg*

Eighteen mice were divided into three groups (Fig. 1E): the healthy mice with Cy7-*Pg* gavage (the gcontrol-*Pg* group, n = 6), the periodontitis mice with Cy7-*Pg* gavage (the gCp-*Pg* group, n = 6) and the healthy control (the gcontrol group, n = 6). The Cy7-*Pg* pellet was resuspended with 2% CMC. For the gcontrol-*Pg* and gCp-*Pg* mice, 100 μL Cy7-*Pg* ($\sim 1 \times 10^9$ CFU) was administered across the oral cavity to

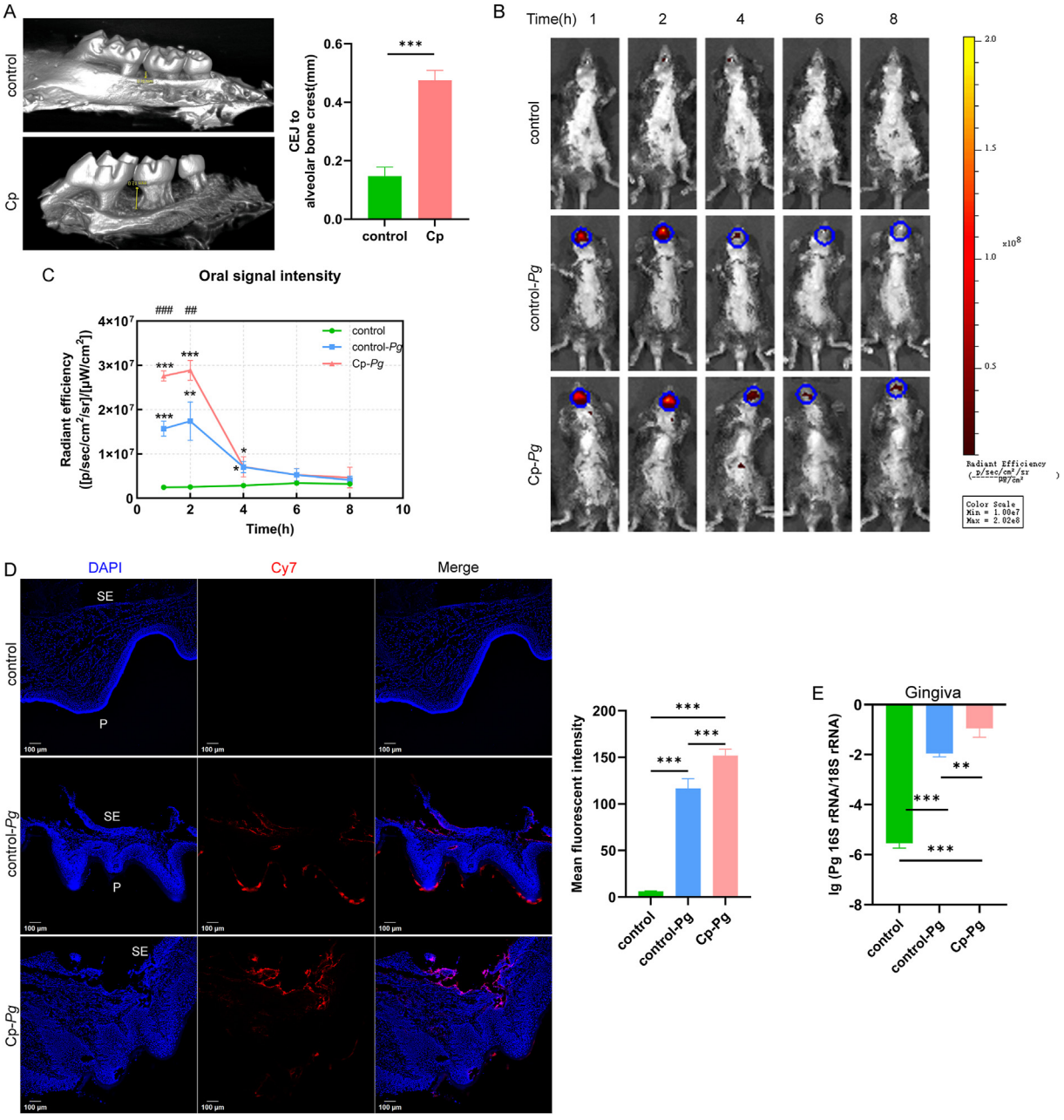

Figure 2 Accumulation of *Pg* in the gingiva upon injection

A: Microcomputed tomography results of the control group and the Cp group, measuring the distance from the alveolar bone crest to CEJ. n = 4 mice per group. B, C: *In vivo* imaging system detection following intra-gingival injection for 8 h n = 3 mice per group. The average signal intensity of oral cavity was calculated within regions of interest with the same size. 1 h, 2 h and 4 h, one-way ANOVA with the Bonferroni test post hoc analysis. 6 h, one-way ANOVA with Tamhane'T2 post hoc analysis since heterogeneity of variance. 8 h, Kruskal-Wallis H test since non-normally distributed. D: Frozen section staining of gingival specimens of the three groups. The graph depicted the mean Cy7 fluorescent intensity of 10 randomly selected sections from 3 mice each group. SE: sulcular epithelium, P: palatal surface of gingiva. One-way ANOVA with Tamhane'T2 post hoc analysis since heterogeneity of variance. E: PCR results of *Pg* 16S rRNA copies in the gingiva of the control, control-*Pg* and Cp-*Pg* group. n = 3 mice per group. Scale bar = 100 μm *$P < 0.05$, **$P < 0.01$, ***$P < 0.001$. For E, *: compared to the control group, $P < 0.05$. **: compared to the control group, $P < 0.01$. ***: compared to the control group, $P < 0.001$. ##: compared to the control-*Pg*, $P < 0.01$. ###: compared to the control-*Pg*, $P < 0.001$. Data are all presented as mean ± SD. CEJ: cementoenamel junction. control-*Pg*: the healthy mice with Cy7-*Pg* injection. Cp: periodontitis mice by ligature. Cp-*Pg*: the periodontitis mice with Cy7-*Pg* injection. *Pg*: *Porphyromonas gingivalis*.

the esophagus using an feeding needle. The gcontrol mice received 100 μL 2% CMC. Each group contained 3 mice at each time point. At 20 min and 200 min, the organs were isolated for examination. The blood and organ samples were harvested and examined in the same way as mentioned above.

Statistical analysis

All data were analyzed using SPSS 25.0 (IBM, Chicago, IL, USA) and graphed with GraphPad Prism 9.5.1 (GraphPad Software, La Jolla, CA, USA). Results were presented as means ± SD. When normally distributed (Shapiro–Wilk test), comparisons were made using the Student's t-test or one-way ANOVA with the Bonferroni test post hoc analysis. In case of heterogeneity of variance, Tamhane'T2 post hoc analysis was used. For comparisons of non-normally distributed data, the Mann-Whitney U test or Kruskal-Wallis H test was utilized. Differences were considered significant at $P < 0.05$.

Results

Greater accumulation of *Pg* in the gingiva with periodontitis upon injection

Before administration of Cy7-*Pg in vivo*, we confirmed that Cy7-*Pg* retained viability, immunomodulatory ability and toxicity (Supplementary Fig. 1). Following three-week ligature, the alveolar bone of Cp mice suffered significant resorption (Fig. 2A).

To figure out the distribution of Cy7-*Pg*, we detected the mice using IVIS continuously for 8 h (Fig. 2B and C). The signal appeared mainly in the mouth and decreased rapidly at 4 h. At 1 h and 2 h, the oral signal intensity for the Cp-*Pg* group was 1.8 times higher than the control-*Pg* group ($P < 0.01$). Six hours later, there were no differences among the three groups. To elucidate *Pg* in situ, the gingiva was collected for frozen sections and PCR. In the confocal images of the control group (Fig. 2D), the sulcus epithelium (SE) was intact. For the control-*Pg* gingiva, the SE was broken at the injection sites, where Cy7 signals concentrated most and became weaker in the deeper. Other Cy7-*Pg* located lateral to the palatal surface. While in the Cp-*Pg* group, less Cy7-*Pg* spilled onto the surface. The mean Cy7 fluorescent intensity of the Cp-*Pg* group was 1.3 times higher than the control-*Pg* group ($P < 0.001$). PCR results demonstrated that *Pg* 16S rRNA copies of the Cp-*Pg* group were 10.0 times higher than the control-*Pg* group ($P < 0.01$) (Fig. 2E). The results of the above three methods demonstrated a higher accumulation of Cy7-*Pg* in situ in the Cp-*Pg* mice than the control-*Pg* mice.

Entry of Cy7-*Pg* into the blood circulation

To illustrate the dynamics of Cy7-*Pg* in the circulation upon injection, PCR for blood samples at these timepoints were performed (Fig. 3). CT = 35 was defined as the limit for detection, thus the detection threshold was 10^4 -10^5 copies/mL. For the control group, no *Pg*-specific DNA copies were detected. Only at 20 min, the quantity of *Pg* DNA in the Cp-*Pg* group was 36.3 times higher than that of the control-*Pg* group ($P < 0.05$), which indicated that the higher accumulation of *Pg* in the gingiva associated with the heavier *Pg* load in the bloodstream. Then between 50 min and 200 min, *Pg* was rapidly cleared, close to the detection threshold.

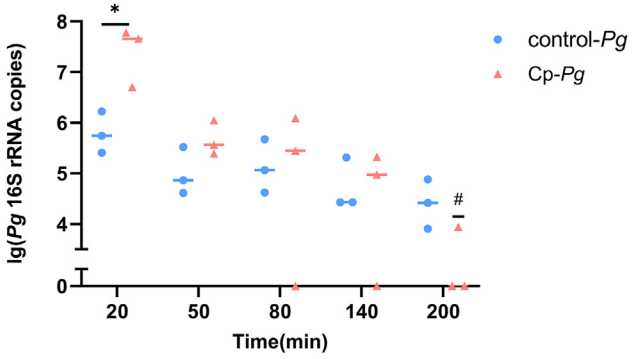

Figure 3 ***Pg* 16S rRNA copies in the blood samples at serial timepoints**
The graph depicted qPCR results of blood samples following *Pg* injection. For comparisons between the two groups (n = 3 per group) at each timepoint, two sample *t* test was performed at 20 min, 50 min and 80 min, while Mann-Whitney U test was used at 140 min and 200 min since the data were not normally distributed. For comparisons between time points within control-*Pg* or Cp-*Pg* group, Kruskal-Wallis H test was used. *: $P < 0.05$. #: compared to the Cp-*Pg* at 20 min, $P < 0.05$. control-*Pg*: the healthy mice with Cy7-*Pg* injection. Cp-*Pg*: the periodontitis mice with Cy7-*Pg* injection. *Pg*: *Porphyromonas gingivalis*.

Translocation of Cy7-*Pg* to distant organs

Considering the biodistribution of *Pg* in distant organs, the liver, kidney and pancreas were isolated *in vitro* for detection at serial timepoints in 3 h after injection. IVIS images showed the fluctuation of Cy7 signals in these organs (Fig. 4). The liver was the organ that Cy7-*Pg* concentrated most and stayed for the longest time, both in the control-*Pg* and Cp-*Pg* group (Fig. 4A). For the former, Cy7 signals peaked at 50 min and then decreased to no difference from the control group. For the Cp-*Pg* mice, Cy7 signals gradually weakened after 80 min, but remained generally highest within 200 min ($P < 0.05$). The kidney and pancreas shared similar Cy7 signal patterns, which were weaker and lasted for the shorter time after the liver (Fig. 5B and C). Signals of the Cp-*Pg* mice were stronger than the control mice within 50 min ($P < 0.05$), while 20 min for the control-*Pg* group ($P < 0.05$).

For further verification, we collected the liver (20 min, 50 min, 80 min and 200 min), kidney (50 min) and pancreas (50 min) for PCR and frozen sections. CT values of organs in the control group with *Pg*-specific primers were all higher than 35. *Pg* DNA was most concentrated in the liver, both in the control-*Pg* ($P < 0.05$) and Cp-*Pg* ($P < 0.001$). The amount of *Pg* DNA was comparable between the kidney and pancreas (Fig. 5A). Besides, compared to the control-*Pg*, the Cp-*Pg* contained more *Pg* DNA in all the three organs

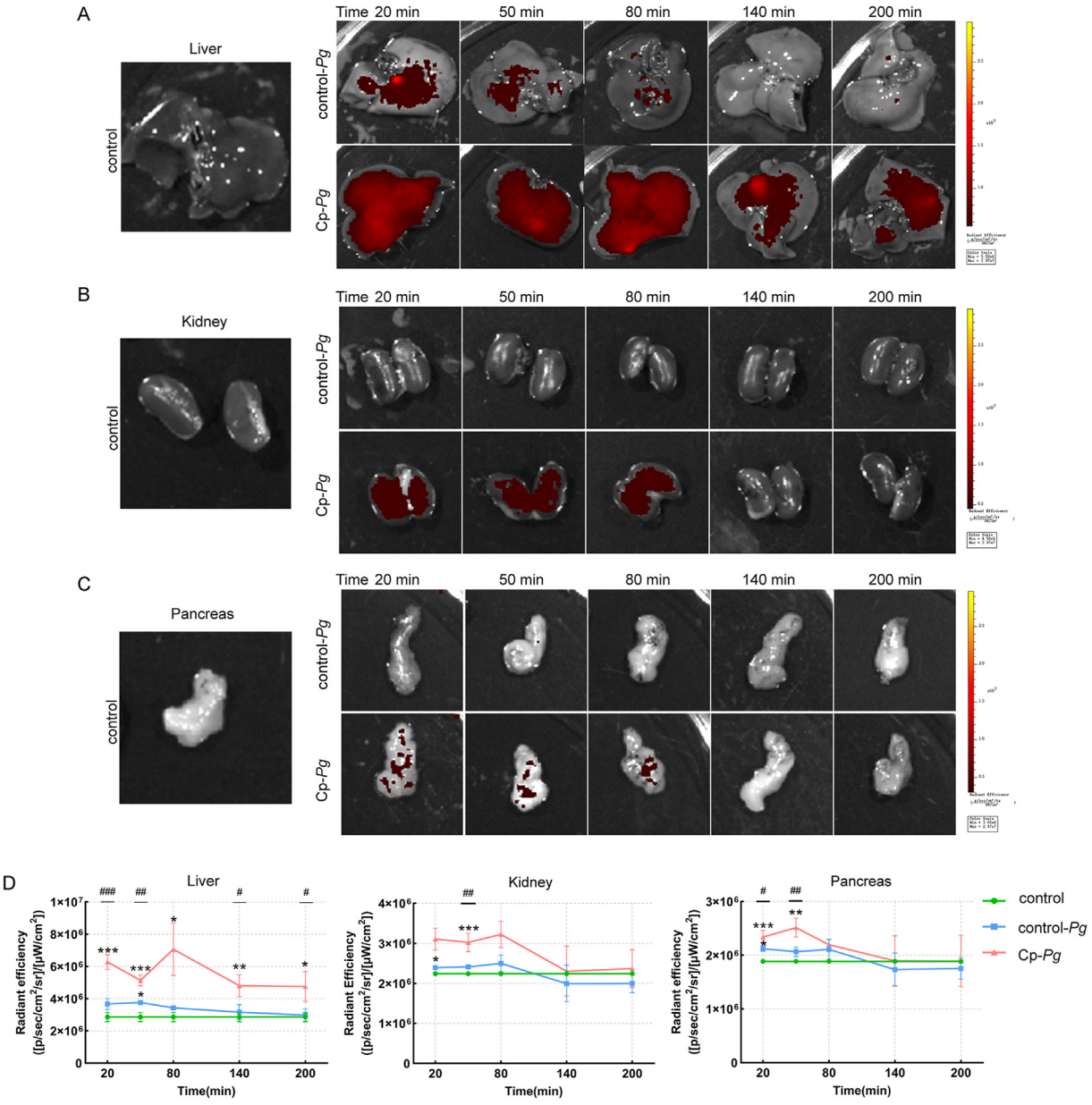

Figure 4 Spatio-temporal distribution of Cy7-*Pg* in multiple organs at serial timepoints
After gingival injection of Cy7-*Pg*, multiple organs (A: liver, B: kidney, C: pancreas) were isolated and placed in order for *in vivo* imaging detection. The graphs depicted the average signal intensity calculated of the three groups. The control-*Pg* and Cp-*Pg* group contained 3 mice at each time points and the control group contained 3 mice. If normally distributed, when variance in homogeneity, one-way ANOVA with the Bonferroni test post hoc analysis was performed, otherwise Tamhane'T2 post hoc analysis was used. Kruskal-Wallis H test was used if nonnormally distributed. Data were shown as mean ± SD. *: compared to the control group, $P < 0.05$. **: compared to the control group, $P < 0.01$. ***: compared to the control group, $P < 0.001$. #: compared to the control-*Pg*, $P < 0.05$. ##: compared to the control-*Pg*, $P < 0.01$. ###: compared to the control-*Pg*, $P < 0.001$. control-*Pg*: the healthy mice with Cy7-*Pg* injection. Cp-*Pg*: the periodontitis mice with Cy7-*Pg* injection. Cy7-*Pg*: *Porphyromonas gingivalis* labeled by cyanine 7.

(Fig. 5B, C and D). Results of liver frozen sections (50 min) were consistent (Fig. 5E and F). Concerning the kidneys and the pancreas, very few Cy7-*Pg* were discovered in the Cp-*Pg* (white arrow heads), while none was found in the control-*Pg* or the control group (Supplementary Fig. 2). The results of above three methods indicated varied duration and signal intensities in these organs. The Cy7 signals in periodontitis mice were generally stronger and lasted longer than healthy controls.

Pg from single oral gavage didn't enter blood via the gut

Despite of liquid-absorbing cotton balls, a small amount of Cy7-*Pg* was inevitably swallowed into the gastrointestinal tract (Fig. 6A), where Cy7-*Pg* might also enter the blood circulation. To illustrate the origin of bacteria in the blood, 100 μL Cy7-*Pg* (~1 × 10^9 CFU, the same amount as the injection) was administered through oral gavage. No

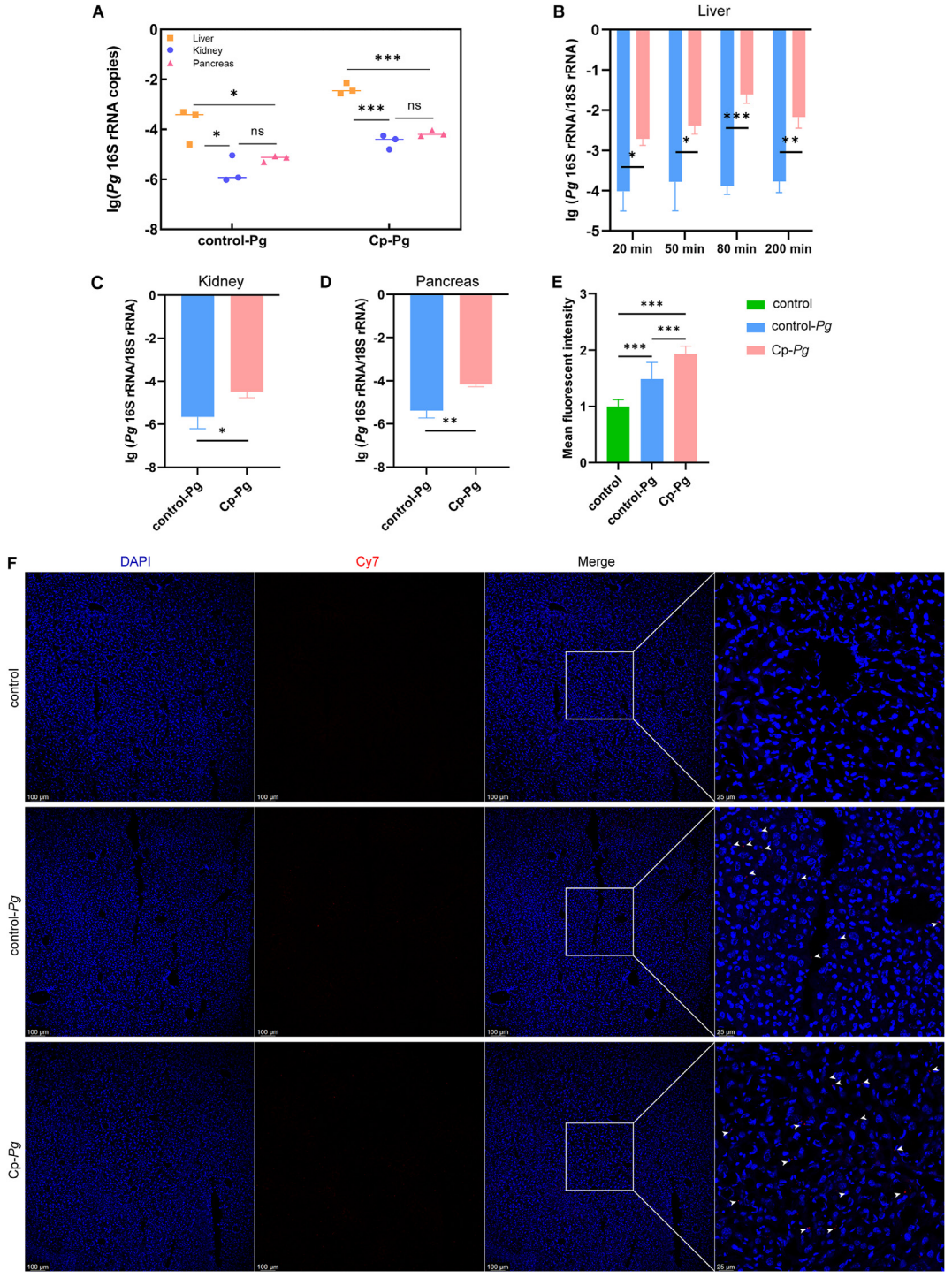

Figure 5 qPCR and frozen sections for *Pg* detection in the multiple organs

A-D: qPCR results of liver (20 min, 50 min, 80 min and 200 min), kidney (50 min) and pancreas (50 min) in the control-*Pg* and Cp-*Pg* groups. n = 3 mice per group at each timepoint. E, F: Frozen sections of liver at 50 min of three groups. The Cp-*Pg* group contained more red dots (Cy7-*Pg*, white arrow heads) than the control-*Pg* group, yet no Cy7-*Pg* was identified in the control group. Mean Cy7 fluorescent signal intensity was calculated in 10 visual fields randomly selected from 3 mice per group. For the three images of each panel from left side, Scale bar = 100 μm; for the image of each panel at right side, Scale bar = 25 μm. Data were all shown as mean ± SD. ns: not significant; *: $P < 0.05$. **: $P < 0.01$. ***: $P < 0.001$. control-*Pg*: the healthy mice with Cy7-*Pg* injection. Cp-*Pg*: the periodontitis mice with Cy7-*Pg* injection. Cy7-*Pg*: *Porphyromonas gingivalis* labeled by cyanine 7.

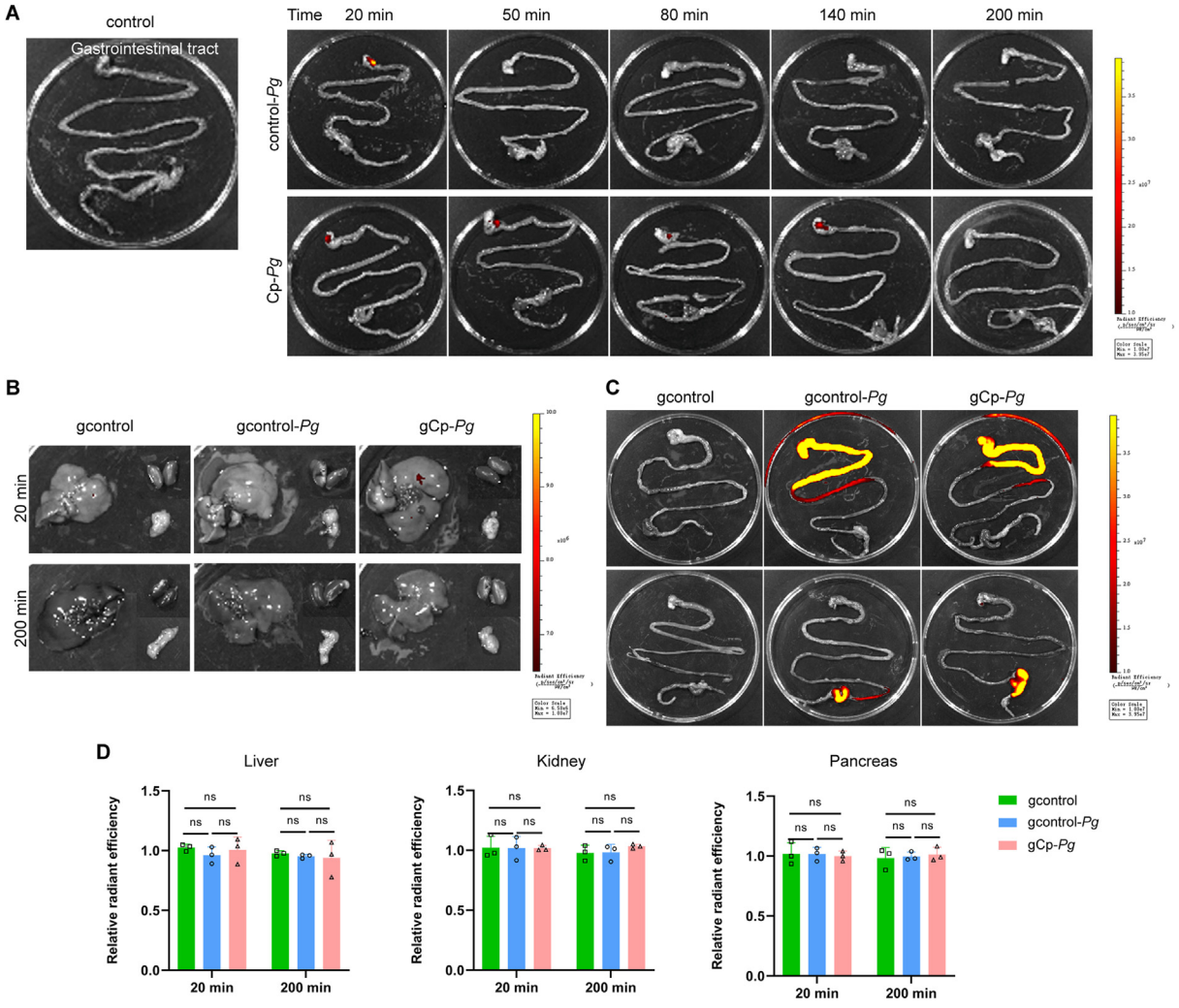

Figure 6 ***Pg*** **from single oral gavage didn't enter blood via gut**

A: IVIS images of the gastrointestinal tract in the control group, control-*Pg* and Cp-*Pg* group following Cy7-*Pg* injection at serial timepoints. B–D: IVIS images of multiple organs of the three groups after oral gavage of Cy7-*Pg* at 20 min and 200 min, with graphs showing the average Cy7 fluorescent intensity. n = 3 mice per group at each timepoint. Data were shown as mean ± SD. ns: not significant. Cy7-*Pg*: *Porphyromonas gingivalis* labeled by cyanine 7. gcontrol: the healthy mice with carboxymethyl cellulose gavage. gcontrol-*Pg*: the healthy mice with Cy7-*Pg* gavage. gCp-*Pg*: the periodontitis mice with Cy7-*Pg* gavage. IVIS: *in vivo* imaging system.

differences of fluorescent intensity were found among the organs in the three groups at 20 min or 200 min (Fig. 6B, C and D). Further, no *Pg*-specific DNA in blood was amplified in the three groups, and CT values of the organ samples using *Pg*-specific primers were all higher than 35. Therefore, the *Pg* detected in the blood originated from the gingiva.

Discussion

Non-communicable diseases, including diabetes, chronic kidney disease and non-alcoholic fatty liver disease, are related to chronic inflammation with unknown etiology. Periodontitis is also a chronic inflammatory disease, which is caused by persistent bacterial infection. This suggests that periodontal pathogens possibly contribute to the systemic inflammation. To illustrate the issue, in this study, live *Pg* was tagged, and tracked from gingiva to distant organs.

PCR and immunological methods have been regularly utilized to detect bacteria, yet without distinguishing the live or dead ones. The foundation of our work was the metabolic labeling of *Pg* with Cy7, which enabled the fluorescence observed to primarily derive from live bacteria. In other words, when the labeled bacteria were dead, the fluorescent signal greatly decreased.[15] GalNAz, the unnatural sugar connecting fluorescent probes, was identified in the O-linked glycoproteins in the membrane[16] and capsular polysaccharide.[14] Once bacteria invade, complement system rapidly recognizes them and forms membrane attack complexes, resulting in bacterial collapse and lysis within minutes. Opsonized bacteria can also be phagocyted and killed intracellularly by macrophages.[17,18] This rupture

of membrane integrity probably leads to decreased fluorescence intensity. Moreover, cell viability, immunomodulatory ability and toxicity of bacteria were not affected by metabolic labeling.

There are three potential pathways for periodontal pathogens to disseminate: hematogenous, oral-pharyngeal and oral-digestive route. Cotton balls prevented *Pg* from inhalation and swallowing, minimizing the interference from the latter two. The similar article was published by Paula-Lima's group.[19] *Pg* (100 μL) was injected into the palatal gingiva, then 45 days later was detected in the serum, cerebro-spinal fluid, and hippocampus via PCR and immunofluorescence. We further excluded the entry to bloodstream from gut with the oral-gavage experiment, which is consistent with previous studies.[20,21] However, via repeated oral inoculations, *Pg* was reported to colonize in the distant organs,[8,22] yet without deciphering translocation routes, which requires further explorations.

The fluctuation of *Pg* was depicted in the three organs via *in vivo* imaging. Similarly, radio-labeled *Pg*-LPS was injected into the palatal gingiva of healthy rats, and concentrated most in the liver at 30 min, with the radioactivity of serum also peaking at this time.[23] These results imply the liver emerges a significant role in the defense against periodontitis-associated infection. It is likely due to the large blood volume and strong innate immunity in the liver.[24] The Kupffer cells mainly and quickly capture free bacteria without opsonization or binding platelets using scavenger receptors when facing a low-level bacteremia.[25]

Furthermore, to evaluate the influence of periodontitis on systemic health, *Pg* was injected into the gingiva of healthy and periodontitis mice with similar forces. For the situ, weaker defense of inflamed gingiva resulted in greater accumulation of *Pg*. Consistently, either bacteria or specific periodontal pathogens were reported more prevalent in the gingiva of patients[26] or rats with periodontitis.[27] *Fn* and *Pg* were even discovered inside the endothelial cells of gingival capillaries in periodontitis patients.[28] As for the bacteremia, previous articles and us both agreed on the heavier bacterial load in the periodontitis group. The prevalence and the magnitude of bacteremia after scaling was significantly higher in periodontitis patients compared to the gingivitis and healthy controls. The number of sites with bleeding on probing, gingival index and plaque index correlated with the magnitude.[29] It is likely due to the ulcerative pocket epithelium, with dilated and proliferated vasculature, making it easier to enter the circulation.[30]

Admittedly, intra-gingival injection amplified the magnitude of periodontal infection. The bacterial magnitude in the blood was 100 CFU/mL[10] for dental procedures and 0.01—32 CFU/mL[29] for daily oral activities. Knowing that one bacterial cell contains about 7 copies of 16S rRNA,[31] thus in our study the average *Pg* load for the control-*Pg* group and the Cp-*Pg* group at 20 min was 8.4×10^4 cells/mL and 3.4×10^6 cells/mL, respectively. Cells/mL should not be converted directly into CFU/mL, since the PCR only determines DNA levels without distinguishing between live and dead bacteria, resulting in the higher cell counts than the actual count. Even though, intra-gingival injection still cannot totally reflect the actual chronic infection process, which is one of the limitations of this study.

Combining the results above, we showed that periodontitis was associated with higher amount of *Pg* accumulation in the gingiva, and entry into the bloodstream following intra-gingival injection. It further led to more *Pg* concentrating in multiple organs, where the duration and magnitude of *Pg* varied. Limitations of this study are listed. On the one side, a single intra-gingival injection still cannot totally reflect the periodontal chronic infectious process. On the other side, the impact of recurrent low-grade infection on distant organs should be further studied. To conclude, we took one step further for illustrating translocation of *Pg* from gingiva to distant organs, and provided more direct evidences for correlations between periodontitis and overall health.

Declaration of competing interest

The authors have no conflicts of interest relevant to this article.

Acknowledgments

This study was supported by grants from Research Foundation of Peking University School and Hospital of Stomatology (PKUSS20220106) and Nature Science Foundation of Beijing (7222227, 7244446).

Appendix A. Supplementary data

Supplementary data to this article can be found online at https://doi.org/10.1016/j.jds.2024.07.009.

References

1. Suzuki S, Sugihara N, Kamijo H, et al. Reasons for tooth extractions in Japan: the second nationwide survey. *Int Dent J* 2022;72:366—72.
2. Kinane DF, Stathopoulou PG, Papapanou PN. Periodontal diseases. *Nat Rev Dis Prim* 2017;3:17038.
3. Curtis MA, Diaz PI, Van Dyke TE. The role of the microbiota in periodontal disease. *Periodontol* 2000 2020;83:14—25.
4. Hajishengallis G. Interconnection of periodontal disease and comorbidities: evidence, mechanisms, and implications. *Periodontol* 2000 2022;89:9—18.
5. Zou Z, Fang J, Ma W, et al. Porphyromonas gingivalis gingipains destroy the vascular barrier and reduce CD99 and CD99L2 expression to regulate transendothelial migration. *Microbiol Spectr* 2023;11:e0476922.
6. Dominy SS, Lynch C, Ermini F, et al. Porphyromonas gingivalis in Alzheimer's disease brains: evidence for disease causation and treatment with small-molecule inhibitors. *Sci Adv* 2019;5:eaau3333.
7. Nagasaki A, Sakamoto S, Chea C, et al. Odontogenic infection by Porphyromonas gingivalis exacerbates fibrosis in NASH via hepatic stellate cell activation. *Sci Rep* 2020;10:4134.
8. Ilievski V, Toth PT, Valyi-Nagy K, et al. Identification of a periodontal pathogen and bihormonal cells in pancreatic islets of humans and a mouse model of periodontitis. *Sci Rep* 2020;10:9976.
9. Horliana AC, Chambrone L, Foz AM, et al. Dissemination of periodontal pathogens in the bloodstream after periodontal procedures: a systematic review. *PLoS One* 2014;9:e98271.

10. Martins CC, Lockhart PB, Firmino RT, et al. Bacteremia following different oral procedures: systematic review and meta-analysis. *Oral Dis* 2024;30:846—54.
11. Lockhart PB, Brennan MT, Sasser HC, Fox PC, Paster BJ, Bahrani-Mougeot FK. Bacteremia associated with toothbrushing and dental extraction. *Circulation* 2008;117:3118—25.
12. Tomas I, Diz P, Tobias A, Scully C, Donos N. Periodontal health status and bacteraemia from daily oral activities: systematic review/meta-analysis. *J Clin Periodontol* 2012;39:213—28.
13. Lin L, Du Y, Song J, Wang W, Yang C. Imaging commensal microbiota and pathogenic bacteria in the gut. *Acc Chem Res* 2021;54:2076—87.
14. Geva-Zatorsky N, Alvarez D, Hudak JE, et al. In vivo imaging and tracking of host-microbiota interactions via metabolic labeling of gut anaerobic bacteria. *Nat Med* 2015;21:1091—100.
15. Wang W, Yang Q, Du Y, et al. Metabolic labeling of peptidoglycan with NIR-II dye enables in vivo imaging of gut microbiota. *Angew Chem Int Ed Engl* 2020;59:2628—33.
16. Laughlin ST, Baskin JM, Amacher SL, Bertozzi CR. In vivo imaging of membrane-associated glycans in developing zebrafish. *Science* 2008;320:664—7.
17. Bjanes E, Nizet V. More than a pore: nonlytic antimicrobial functions of complement and bacterial strategies for evasion. *Microbiol Mol Biol Rev* 2021;85:e00177. -20.
18. Heesterbeek D, Angelier ML, Harrison RA, Rooijakkers S. Complement and bacterial infections: from molecular mechanisms to therapeutic applications. *J Innate Immun* 2018;10:455—64.
19. Diaz-Zuniga J, More J, Melgar-Rodriguez S, et al. Alzheimer's disease-like pathology triggered by Porphyromonas gingivalis in wild type rats is serotype dependent. *Front Immunol* 2020;11:588036.
20. Abed J, Maalouf N, Manson AL, et al. Colon cancer-associated Fusobacterium nucleatum may originate from the oral cavity and reach colon tumors via the circulatory system. *Front Cell Infect Microbiol* 2020;10:400.
21. Nakajima M, Arimatsu K, Kato T, et al. Oral administration of P. gingivalis induces dysbiosis of gut microbiota and impaired barrier function leading to dissemination of enterobacteria to the liver. *PLoS One* 2015;10:e0134234.
22. Yao C, Lan D, Li X, Wang Y, Qi S, Liu Y. Porphyromonas gingivalis is a risk factor for the development of nonalcoholic fatty liver disease via ferroptosis. *Microb Infect* 2023;25:105040.
23. Fujita M, Kuraji R, Ito H, et al. Histological effects and pharmacokinetics of lipopolysaccharide derived from Porphyromonas gingivalis on rat maxilla and liver concerning with progression into non-alcoholic steatohepatitis. *J Periodontol* 2018;89:1101—11.
24. Jenne CN, Kubes P. Immune surveillance by the liver. *Nat Immunol* 2013;14:996—1006.
25. Broadley SP, Plaumann A, Coletti R, et al. Dual-track clearance of circulating bacteria balances rapid restoration of blood sterility with induction of adaptive immunity. *Cell Host Microbe* 2016;20:36—48.
26. Choi YS, Kim YC, Jo AR, et al. Porphyromonas gingivalis and dextran sulfate sodium induce periodontitis through the disruption of physical barriers in mice. *Eur J Inflamm* 2013;11:419—31.
27. Choi YS, Kim YC, Ji S, Choi Y. Increased bacterial invasion and differential expression of tight-junction proteins, growth factors, and growth factor receptors in periodontal lesions. *J Periodontol* 2014;85:e313—22.
28. Rajakaruna GA, Negi M, Uchida K, et al. Localization and density of Porphyromonas gingivalis and Tannerella forsythia in gingival and subgingival granulation tissues affected by chronic or aggressive periodontitis. *Sci Rep* 2018;8:9507.
29. Forner L, Larsen T, Kilian M, Holmstrup P. Incidence of bacteremia after chewing, tooth brushing and scaling in individuals with periodontal inflammation. *J Clin Periodontol* 2006;33:401—7.
30. Vitkov L, Singh J, Schauer C, et al. Breaking the gingival barrier in periodontitis. *Int J Mol Sci* 2023;24:4544.
31. Rupf S, Merte K, Eschrich K. Quantification of bacteria in oral samples by competitive polymerase chain reaction. *J Dent Res* 1999;78:850—6.